

# Optically Driven Terahertz Wave Modulator Using Ring-Shaped Microstripline With GaInAs Photoconductive Mesa Structure

Satoshi Yamasaki, Akio Yasui, Tomohiro Amemiya, *Member, IEEE*, Kentaro Furusawa, *Member, IEEE*, Shinsuke Hara, *Member, IEEE*, Issei Watanabe, Atsushi Kanno, *Member, IEEE*, Norihiko Sekine, *Member, IEEE*, Zhichen Gu, Nobuhiko Nishiyama, *Senior Member, IEEE*, Akifumi Kasamatsu, and Shigehisa Arai, *Fellow, IEEE*

**Abstract**—To improve wireless communications systems, it is desirable to seamlessly combine fiber-based optical and terahertz wireless communications systems. In this paper, we demonstrate a waveguide optically driven terahertz wave modulator using a ring-shaped microstripline with a GaInAs photoconductive mesa structure. In this device, terahertz wave modulation is performed by controlling the photo-generated carriers in the GaInAs mesa. As a result, a maximum extinction ratio of 16.8 dB in the terahertz band was obtained with a light irradiation of 15 dBm (32 mW), and the 3 dB modulation bandwidth was approximately 170 MHz.

**Index Terms**—Terahertz, III–V semiconductor, waveguide.

## I. INTRODUCTION

THE terahertz band, which is defined as the frequency range between 100 GHz and 10 THz, has been the focus of much attention due to its potential to enable numerous applications in the medical, chemical, biological, and information communication fields [1]–[7].

In particular, it is anticipated that wireless communications in the terahertz band will contribute toward solving several important problems in current wireless systems, such as spectrum scarcity and system capacity limitations. In 2002, a 120-GHz-band terahertz-wave photonic wireless link was demonstrated for 10 Gb/s data transmission [8], [9]. In recent years, 100 Gbit/s data transmissions at 237.5 GHz using quadrature amplitude modulation (QAM) have now been achieved. In

Manuscript received October 1, 2016; revised January 3, 2017; accepted January 26, 2017. This work was supported by the JST CREST, JSPS KAKENHI Grants #25709026, #15H05763, and #16H06082.

S. Yamasaki, A. Yasui, and Z. Gu are with the Department of Electrical and Electronic Engineering, Tokyo Institute of Technology, Tokyo 152-8550, Japan (e-mail: yamasaki.s.ae@m.titech.ac.jp; yasui.a.ab@m.titech.ac.jp; gu.z.ab@m.titech.ac.jp).

T. Amemiya, N. Nishiyama, and S. Arai are with the Department of Electrical and Electronic Engineering, Tokyo Institute of Technology, Tokyo 152-8550, Japan, and also with the Institute of Innovative Research, Tokyo Institute of Technology, Tokyo 152-8552, Japan (e-mail: amemiya.t.ab@m.titech.ac.jp; nishiyama@ee.e.titech.ac.jp; arai@pe.titech.ac.jp).

K. Furusawa, S. Hara, I. Watanabe, A. Kanno, N. Sekine, and A. Kasamatsu are with the Advanced ICT Research Institute, National Institute of Information and Communications Technology, Tokyo 184-8795, Japan (e-mail: kfurusawa@nict.go.jp; s-hara@nict.go.jp; issei@nict.go.jp; kanno@nict.go.jp; nsekine@nict.go.jp; kasa@nict.go.jp).

Color versions of one or more of the figures in this paper are available online at <http://ieeexplore.ieee.org>.

Digital Object Identifier 10.1109/JSTQE.2017.2662660

this system, a uni-traveling-carrier photodetector (UTC-PD) that utilized only electrons as active carriers was used as a high-speed terahertz generator [10], [11].

At the same time, as they support high capacity data rates, fiber-based wired optical communications systems are being installed in long-haul networks. A large number of waveguide photonic devices will be required in order to make such systems at a reasonable cost and in a limited space.

Optically-driven terahertz wave modulators are indispensable elements used to seamlessly connect wireless terahertz communications systems and wired optical communications systems. They must, by necessity, have the form of a GaInAsP/InP waveguide because they must be monolithically combined with other conventional photonic devices such as semiconductor lasers, optical amplifiers, and modulators [12]. Conventional optically-driven terahertz wave modulators using photo-generated carriers in semiconductors, however, cannot meet the above requirement because they have the form of Si-based parallel plate waveguide [13], GaAs-based active metamaterials [14], [15], and GaInAs-based bulk wafers [16].

Therefore, in this paper, we have proposed and investigated InP-based waveguide optically-driven terahertz wave modulators using a ring-shaped microstripline with a GaInAs photoconductive mesa structure. This modulator is compatible with standard fabrication processes for photonic integrated circuits (PICs) [17], and is easily integrated with other InP-based optical devices. The paper is organized as follows. First, the concept of the device and its theoretical foundation are provided in Section II. The fabrication processes for the device are explained in Section III. Sections IV and V describe the operating characteristics of the device, and provides the static and dynamic terahertz-wave transmission dependencies based on the input power of the incident light. Finally, Section VI concludes the paper.

## II. CONCEPT OF WAVE MODULATION AND THEORETICAL ANALYSIS

Fig. 1 shows a schematic diagram of our waveguide optically-driven terahertz wave modulators. In the device, an input terahertz wave propagates through a ring-shaped Au/SiO<sub>2</sub>/Au microstripline with a gap consisting of an undoped GaInAs/InP mesa structure.

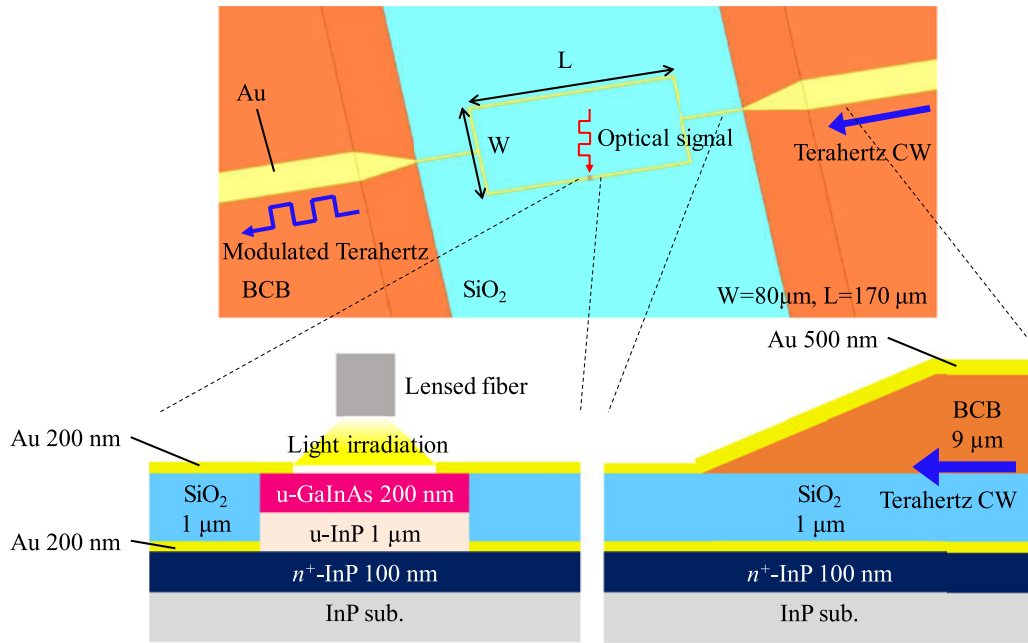


Fig. 1. Waveguide optically-driven terahertz wave modulators using ring-shaped microstripline with GaInAs photoconductive mesa structure.

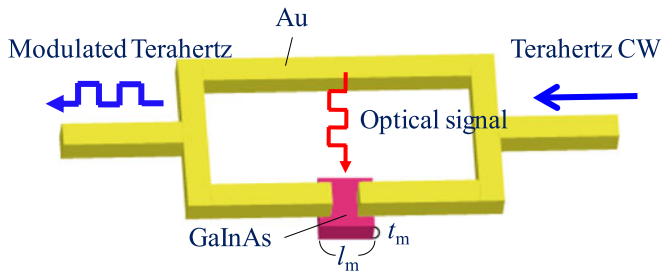


Fig. 2. Enlarged view of ring-shaped microstripline with GaInAs photoconductive mesa in device.

The ring-shaped microstripline described in this paper is a type of antenna operating in the terahertz band [18]. When the frequency of an incident terahertz wave corresponds to the resonance frequency of the ring-shaped microstripline, the device shows a radiation mode and does not transmit the incident terahertz wave. Under this condition, the GaInAs mesa works as a capacitance for the terahertz wave. When optical signal ( $\lambda = 1.55 \mu\text{m}$ ) is irradiated to the mesa (see Fig. 2), the mesa is metallized for terahertz waves by photo-generated carriers. As a result, the resonance of the ring-shaped microstripline disappears and the device transfers from a radiation mode to a transmission mode. Note that the photon energy of the optical signals ( $=0.8 \text{ eV}$ ) is larger than the band gap energy of GaInAs ( $=0.75 \text{ eV}$ ). In this way, the terahertz-band input signals can be modulated as the same pattern of the optical signals [19].

The resonance frequency can be controlled by scaling the ring. Although the center frequency was set to 300 GHz in this study, it is possible to operate at the frequency of more than 1 THz in the same principle.

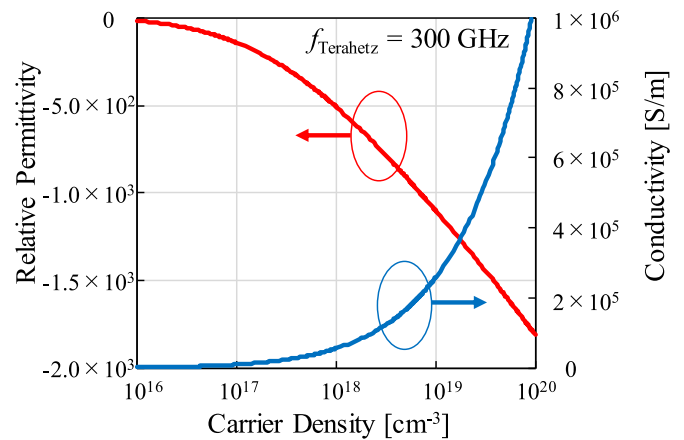


Fig. 3. Calculated relative permittivity and electrical conductivity of a semiconductor material GaInAs as a function of frequency  $f$  and the generated free carrier density.

The modulation properties of the device are extremely dependent on the conduction characteristics of the GaInAs for the terahertz wave. Therefore, we first calculated the constitutive parameters (i.e. the relative permittivity and electrical conductivity) of the GaInAs semiconductor material as a function of free carrier density  $N$  at a frequency of 300 GHz using the Drude model [20]. The results are shown in Fig. 3. Because of the skin effect, the relative permittivity of the GaInAs showed a large negative value with an increase in the carrier density. On the other hand, the electrical conductivity of the GaInAs drastically increased as the carrier density increased. These results indicate that the GaInAs behaves as a metal for terahertz waves.

Using the calculated characteristics of GaInAs as stated above, the device characteristics were analyzed. Considering

TABLE I  
SIMULATION PARAMETERS USED FOR ANALYZING  
THE DEVICE CHARACTERISTICS

Parameters	<i>Sym.</i>	Values
Electron mobility †	$\mu_e (N)$	$\frac{11.300}{1 + \left(\frac{N}{1.69 \times 10^{17}}\right)^{0.436}} [\text{cm}^2/\text{Vs}]$
Wavelength of the optical signal	$\lambda$	1.55 [ $\mu\text{m}$ ]
Radius of spot size	$r_s$	4 [ $\mu\text{m}$ ]
Absorption coefficient of GaInAs	$\alpha$	6,000 [ $\text{cm}^{-1}$ ]
Reflectivity at surface of GaInAs	$R$	0.3
Length of one side of GaInAs mesa	$l_m$	3.5 [ $\mu\text{m}$ ]
Thickness of GaInAs mesa	$t_m$	200 [nm]
Initial doping of GaInAs mesa	$N_0$	$5 \times 10^{16} [\text{cm}^{-3}]$
Recombination coefficient	$B$	$0.79 \times 10^{-10} [\text{cm}^3/\text{s}]$
Short side of rectangle ring	$W$	80 [ $\mu\text{m}$ ]
Long side of rectangle ring	$L$	170 [ $\mu\text{m}$ ]

† The equation for electron mobility used in the simulation was determined by fitting experimental data [21], [22].

carrier recombination, the carrier density  $N(t)$  inside the GaInAs mesa can be written as follows:

$$\frac{dN(t)}{dt} = \Delta N - \frac{N(t) - N_0}{\tau(N(t))}, \quad (1)$$

where  $\tau(N) = (BN)^{-1}$  is the carrier lifetime,  $N_0$  is initial doping concentration of the GaInAs mesa, and  $\Delta N$  is the photo-induced carrier density per unit time. In the device, the modulated optical signals are irradiated from a lensed optical fiber onto the mesa above the device. Therefore, assuming that the radius of the fiber  $r_s$  is the same as that of the irradiation spot size,  $\Delta N$  in (1) can be derived as follows:

$$\Delta N = N_p \frac{l_m^2}{\pi r_s^2} (1 - R) (1 - e^{-\alpha t_m}) \frac{1}{l_m^2 t_m}, \quad (2)$$

where  $l_m$  and  $t_m$  are the length of one side and the thickness of the square mesa structure, respectively (see Fig. 2),  $\alpha$  is the absorption coefficient of GaInAs, and  $R$  is the surface reflectivity for incident light. Additionally,  $N_p$  is the number of incident photons per unit time, as given by the following equation:

$$N_p = \frac{x_{\text{in}}}{hc/\lambda}, \quad (3)$$

where  $x_{\text{in}}$  and  $\lambda$  are the optical power and wavelength of the incident light, respectively,  $h$  is the Plank constant, and  $c$  is the speed of light in vacuum. All of the parameters used in this simulation are summarized in Table I.

Using (1)–(3), we analyzed the transmission characteristics of the device for a 300 GHz terahertz wave (i.e. S parameter  $|S_{21}|$ ) with and without wavelength 1.55  $\mu\text{m}$  CW light using a three-dimensional commercial electromagnetic field simulator HFSS (ver. 15.0, Ansys, Inc.).

Fig. 4 shows the simulated transmission characteristics of the whole device without input light (red line) and with input light present with an optical power of 15 dBm (blue line). In this study, the center frequency of the band-stop filter was set to 300 GHz by designing the ring size shown in Fig. 1 to have a width  $W$  of 80  $\mu\text{m}$  and a length  $L$  of 170  $\mu\text{m}$ .

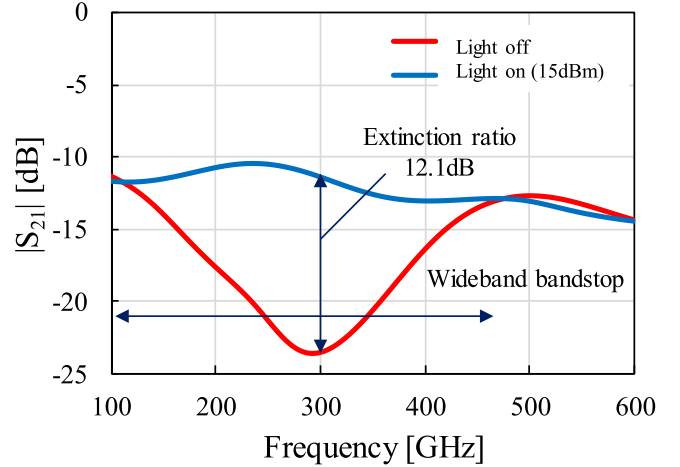


Fig. 4. Calculated transmission characteristics of the device for 300 GHz terahertz wave without input light (red line) and with input light of 15 dBm (blue line).

When there was no input light signal present, the device operated as an ultra-wideband band-stop filter and produced an attenuation of  $-23$  dB at 300 GHz, which corresponds to the center frequency of the band-stop filter. On the other hand, when the input light signal was present, the device was transparent to terahertz waves because the stopband was short-circuited by the excited carriers inside the GaInAs mesa. Based on these results, a magnitude of 12.1 dB switching change in the propagation intensity (i.e. extinction ratio) can be expected at 250–350 GHz frequency. The input optical power dependence of transmission will be shown in Fig. 7 in the next section with measurement results.

### III. FABRICATION PROCESS

We fabricated a prototype device to validate the results of the simulation, as shown in Fig. 5. First, an un-doped InP layer (1  $\mu\text{m}$  thick) and an undoped  $\text{Ga}_{0.47}\text{In}_{0.53}\text{As}$  layer (200 nm thick) were grown on a  $n$ -InP substrate ( $6 \times 10^{18} \text{cm}^{-3}$ ) using the metal organic chemical vapor deposition (MOCVD) method (step 1 in Fig. 5). Next, a photoconductive mesa structure was formed on the wafer using reactive-ion etching and photolithography (step 2 in Fig. 5). Then, a 1- $\mu\text{m}$ -thick  $\text{SiO}_2$  layer was deposited onto the entire substrate after a ground electrode was formed (steps 3–4 in Fig. 5). After removing the  $\text{SiO}_2$  on top of the mesa, the ring-shaped microstripline was formed using a photolithography and lift-off process (steps 5–6 in Fig. 5). Finally, a straight microstripline for the terahertz waves was fabricated on the device surface followed by the formation of a sloped benzocyclobutene (BCB) layer (steps 7–8 in Fig. 5). The thickness of the BCB layer was set to 9  $\mu\text{m}$  in order to facilitate impedance matching.

Fig. 6 shows an optical microscope view of the entire device. The dimensions of the ring were identical to those used in the simulation in the previous sections. For input and output of the terahertz signal, GSG type electrical pads were used with a design under consideration of impedance matching.

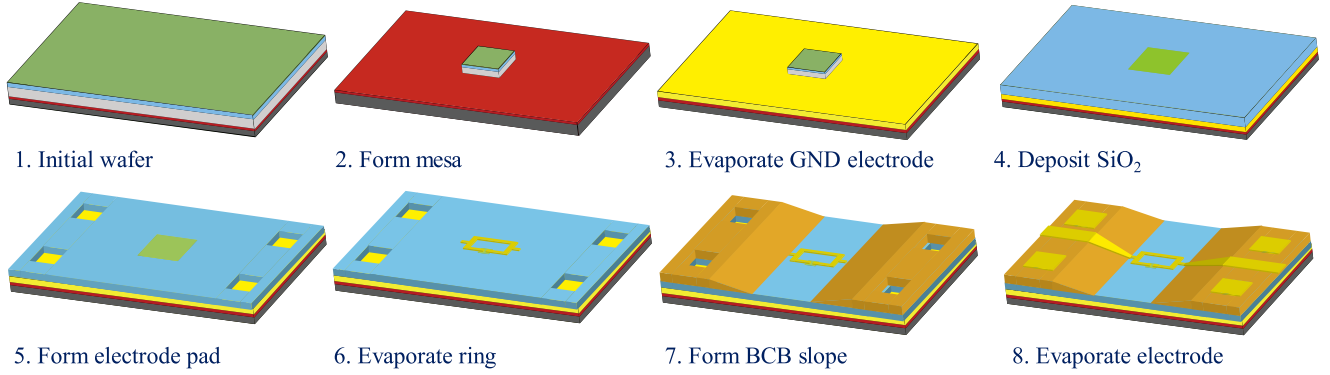


Fig. 5. Fabrication process for the device. The ring-shaped microstripline with GaInAs photoconductive mesa was prepared using photolithography and lift-off process.

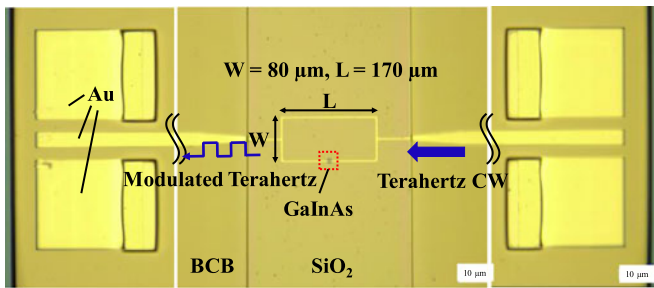


Fig. 6. Plan view of waveguide optically-driven terahertz wave modulators observed with optical microscopy.

#### IV. STATIC CHARACTERISTICS OF DEVICE

The S parameters, which represent the static characteristics of the fabricated device, were first measured using a vector network analyzer (VNA, Keysight PNA-X) that acted as both the signal generator and receiver. The calibration up to the probes (Cascade Microtech, i325-T-GSG-75) was performed using an impedance standard substrate. It should be noted that a frequency extender was used to expand the target frequency range to 220–330 GHz. The measured S-parameters include the coupling to the terahertz waveguide, however, we consider the coupling is almost transparent because the waveguide structure was set to facilitate impedance matching.

The measurement and calculation results of  $|S_{21}|$  with different optical powers are shown in Fig. 7. It can be seen that parameter  $|S_{21}|$  increases as the optical power increases, as expected.

The measurement and simulation results of the frequency characteristics are shown in Fig. 8 using solid and dotted lines, respectively. The change in  $|S_{21}|$  was induced by the switching ON/OFF of the light irradiation ( $\lambda = 1.52 \mu\text{m}$ ) through the lensed fiber. As a result, a maximum extinction ratio of 16.8 dB was obtained at 287 GHz, which shows that our design is capable of realizing the modulation between optical and terahertz waves (On the other hand, measured  $|S_{11}|$  had almost a constant value of  $-10$  dB at 287 GHz regardless of light irradiation).

The differences between the measurement and simulation results were caused by the following two facts. The first is the effects of the parasitic components, such as the electrode pads,

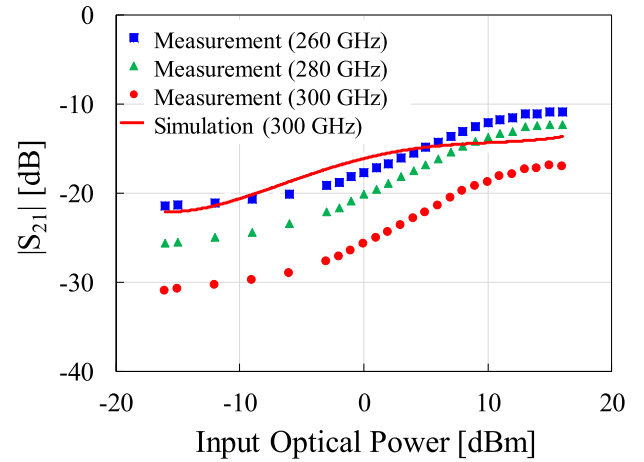


Fig. 7. Measurement and calculation results of  $|S_{21}|$  with different optical powers.

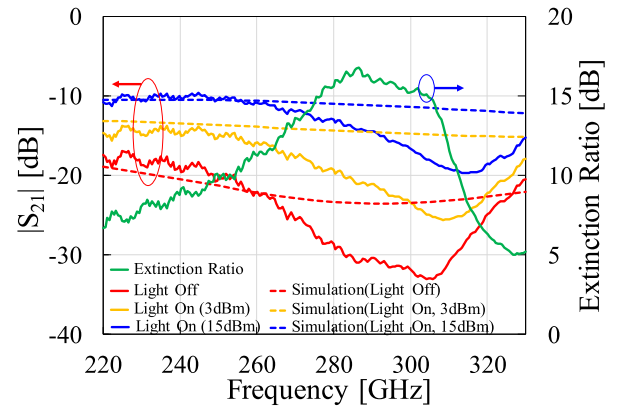


Fig. 8. Measurement and simulation results of transmission characteristics of device for terahertz waves.

which we did not consider in the transmission simulation in the Section II. In the simulation, electromagnetic waves are directly excited in the input waveguide without including the electrode pads. The second is due to fabrication error. Although we assumed the length of one side of the GaInAs mesa to be  $3.5 \mu\text{m}$  in the simulation, it is actually around  $4 \mu\text{m}$  in the experiment.

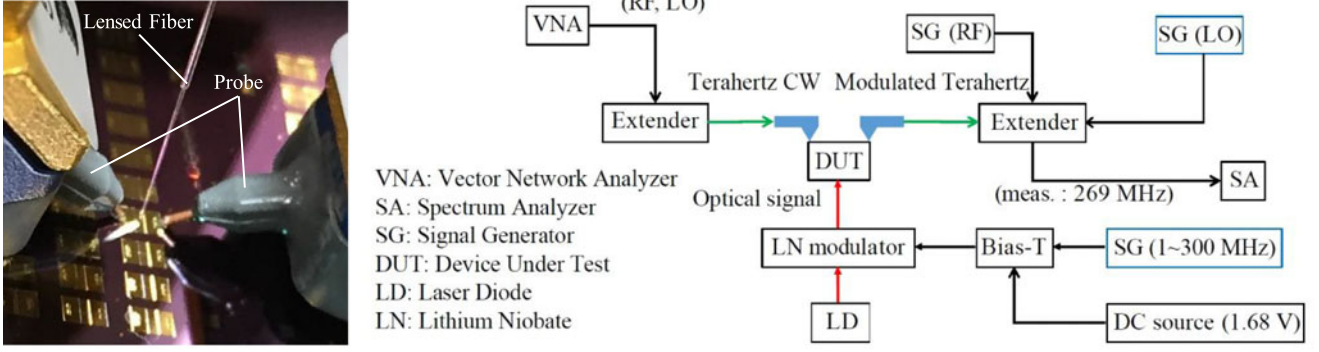


Fig. 9. Experimental setup for measuring dynamic transmission characteristics of device.

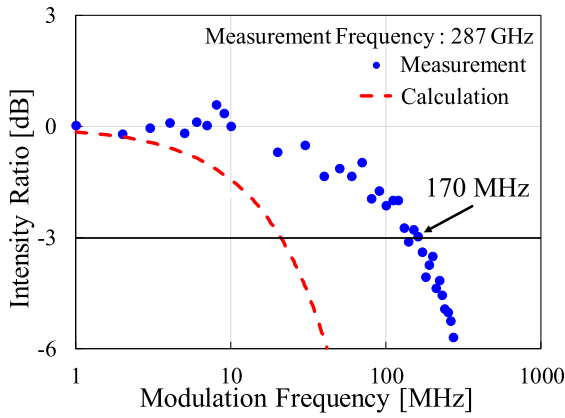


Fig. 10. Dynamic characteristics of the device.

## V. DYNAMIC CHARACTERISTICS OF DEVICE

The dynamic response characteristic of the fabricated device was also measured using the measurement system shown in Fig. 9. A lithium niobate (LN) modulator was used for modulating the optical wave (1–300 MHz, sinusoidal) from a laser diode (TSL-510, Santec). A frequency of 287 GHz was chosen for the terahertz carrier in order to obtain the largest available extinction ratio based on the measurement results shown in Fig. 8. The VNA was only used as a signal generator during this measurement. The output terahertz wave was down-converted to an adjustable intermediate frequency (IF) based on the heterodyne method using a local oscillator (LO). The power of the down-converted modulation sideband was then measured by using a spectrum analyzer. The frequency of LO was tuned with the optical modulation frequency so as to maintain the sideband signal at a constant frequency (269 MHz). This allows us to directly extract the power response of DUT at a given optical modulation frequency, without being affected by the entire system response (i.e. frequency response of the IF bandpass filter itself).

The measurement results are shown in Fig. 10 where the intensity decreases as the modulation frequency increases. As a result, the 3 dB modulation bandwidth was approximately 170 MHz. In order to consider the experimental results above, a theoretical analysis based on the rate equation was performed. In the simulation, the carrier density in the GaInAs mesa was

firstly investigated with the intensity-modulated optical signal. Since the carrier generation speed in the GaInAs mesa is much faster than the carrier extinction speed, only the carrier density during the falling of the optical signal was considered. The carrier density  $N(t)$  can be derived by the following equation:

$$\frac{dN(t)}{dt} = -\frac{N(t) - N_0}{\tau(N(t))}, \quad (4)$$

where  $\tau(N)$  is the carrier lifetime and  $N_0$  is the initial doping concentration of the GaInAs mesa (see Table I for each parameter). After obtaining  $N(t)$  for each modulation frequency, a dynamic response of the terahertz wave was then estimated from Fig. 7.

The calculated modulation-frequency-dependent extinction ratio is shown in Fig. 10 as the dotted line. The measurement bandwidth is wider than what we obtained from the calculation. This phenomenon was attributed to the surface recombination of the GaInAs, which was not considered in our analysis.

One way to enhance the modulation bandwidth is to apply a bias to the GaInAs mesa for removing the photo-generated carriers. Fig. 11(a) shows the schematic image of a modified device structure for high-speed operation, where an electrode is attached on the top of the mesa and a reverse bias is applied between the top u-GaInAs layer and the bottom n<sup>+</sup>-InP layer. In the simulation, we used a three-dimensional TCAD device simulator to calculate a distribution of photo-generated electron density around the mesa under a given reverse bias (Fig. 11(b) depicts one example with the reverse bias of  $-1$  V). For the analysis, we took into consideration the Poisson equation, electron and hole continuity equation, parallel electric field-dependent mobility model, concentration-dependent carrier mobility model, Shockley-Read-Hall recombination model, material-dependent band parameter model, and Fermi-Dirac statistics model.

Fig. 11(c) shows the time dependence of the electron density in the mesa (red point in Fig. 11(b)) calculated with the reverse bias of  $-1$  V and light input of  $50$  kW/cm<sup>2</sup>. Electron accumulation and extinction speeds are  $5 \times 10^{17}$  cm<sup>-3</sup> and 3 ns, respectively. This result indicates that the operation speed over 1 GHz can be achieved with this modulator. On the basis of the simulation results, we finally estimated modulation bandwidth (see Fig. 12) using a three-dimensional electromagnetic field

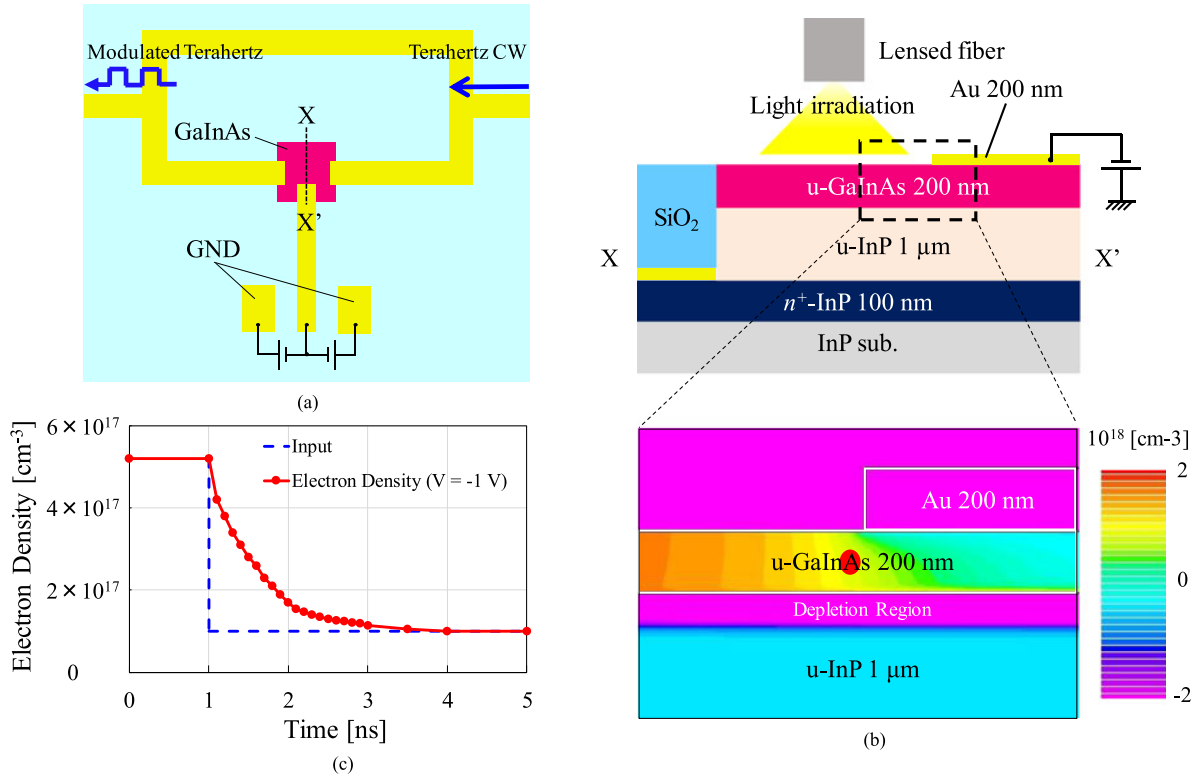


Fig. 11. (a) Schematic image of modified device structure for high speed operation, (b) Example of photo-generated electron density calculation, (c) Time dependence of the electron density.

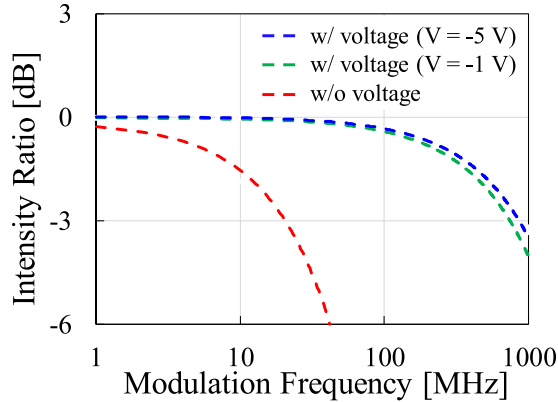


Fig. 12. Modulation bandwidth with applying voltage.

simulator HFSS. As a result, the modulation bandwidth could be increased to 1 GHz with the reverse bias of  $-5$  V.

## VI. SUMMARY

In this paper, a waveguide-type optically-driven terahertz wave modulator with a ring-shaped microstripline structure was demonstrated. The extinction ratios obtained from the simulation and measurements were 12.1 dB and 16.8 dB, respectively, which showed that our design was well suited for terahertz wave modulation application. However, the experiment also demonstrated a modulation bandwidth of 170 MHz which we assume was limited by the carrier lifetime of GaInAs. We believe that applying high voltage during operation of the device

can increase the modulation bandwidth by removing the generated carriers during the fall time of the terahertz wave.

## REFERENCES

- [1] P. H. Siegel, "Terahertz technology," *IEEE Microw. Theory Techn.*, vol. 50, no. 3, pp. 910–928, Mar. 2002.
- [2] R. M. Woodward *et al.*, "Terahertz pulse imaging in reflection geometry of human skin cancer and skin tissue," *Phys. Med. Biol.*, vol. 47, pp. 3853–3863, 2002.
- [3] K. Kawase, Y. Ogawa, Y. Watanabe, and H. Inoue, "Non-destructive terahertz imaging of illicit drugs using spectral fingerprints," *Opt. Express*, vol. 11, no. 20, pp. 2549–2554, 2003.
- [4] W. Withayachumnankul *et al.*, "T-ray sensing and imaging," *Proc. IEEE*, vol. 95, no. 8, pp. 1528–1558, Aug. 2003.
- [5] P. Siegel, "Terahertz technology in biology and medicine," *IEEE Trans. Microw. Theory Techn.*, vol. 52, no. 10, pp. 2438–2447, Oct. 2004.
- [6] T. Nagatsuma, "Terahertz technologies: Present and future," *IEICE Electron. Express*, vol. 8, no. 14, pp. 1127–1142, 2011.
- [7] J. F. O'Hara, W. Withayachumnankul, and I. Al-Naib, "A review on thin-film sensing with terahertz waves," *J. Infrared, Millim., THz Waves*, vol. 33, no. 3, pp. 245–291, 2012.
- [8] T. Minotani, A. Hirata, and T. Nagatsuma, "A broadband 120-GHz Schottky-Diode receiver for 10-Gbit/s wireless links," *IEICE Trans. Electron.*, vol. E86-C, no. 8, pp. 1501–1505, 2003.
- [9] A. Hirata *et al.*, "120-GHz-band millimeter-wave photonic wireless link for 10-Gb/s data transmission," *IEEE Trans. Microw. Theory Techn.*, vol. 54, no. 5, pp. 1937–1942, May 2006.
- [10] H.-J. Song *et al.*, "24 Gbit/s data transmission in 300 GHz band for future terahertz communications," *Electron. Lett.*, vol. 48, no. 15, pp. 953–954, 2012.
- [11] S. Koenig *et al.*, "Wireless sub-THz communication system with high data rate," *Nature Photon.*, vol. 7, pp. 977–981, 2013.
- [12] R. Nagarajan *et al.*, "Large-scale photonic integrated circuits," *IEEE J. Sel. Topics Quantum Electron.*, vol. 11, no. 1, pp. 50–65, Jan./Feb. 2005.
- [13] D. G. Cooke and P. U. Jepsen, "Optical modulation of terahertz pulses in a parallel plate waveguide," *Opt. Express*, vol. 16, no. 19, pp. 15123–15129, 2008.

- [14] W. J. Padilla, A. J. Taylor, C. Highstrete, M. Lee, and R. D. Averitt, "Dynamical electric and magnetic metamaterial response at terahertz frequencies," *Phys. Rev. Lett.*, vol. 96, no. 10, 2006, Art. no. 107401.
- [15] H.-T. Chen *et al.*, "Ultrafast optical switching of terahertz metamaterials fabricated on ErAs/GaAs nanoisland superlattices," *Opt. Lett.*, vol. 32, no. 12, pp. 1620–1622, 2007.
- [16] M. Shirao *et al.*, "Preliminary experiment on direct media conversion from a 1.55  $\mu\text{m}$  optical signal to a sub-terahertz wave signal using photon-generated free carriers," *Jpn. J. Appl. Phys.*, vol. 48, no. 9, 2009, Art. no. 090203.
- [17] J. J. G. M. van der Tol, Y. S. Oei, U. Khaliq, R. Nötzel, and M. K. Smit, "InP-based photonic circuits: Comparison of monolithic integration techniques (review paper)," *Prog. Quantum Electron.*, vol. 34, no. 4, pp. 135–172, 2010.
- [18] S. Ramya and I. Srinivasa Rao, "Design of compact ultra-wideband microstrip bandstop filter using split ring resonator," in *Proc. IEEE Int. Conf. Commun. Signal Process.*, 2015, pp. 105–108.
- [19] S. Yamasaki *et al.*, "Waveguide optical-to-THz signal converter using ring-shaped microstripline," in *Proc. Conf. Lasers Electro-Opt.*, 2016, Paper JTh2A-57.
- [20] R. Ulbricht, E. Hendry, J. Shan, T. F. Heinz, and M. Bonn, "Carrier dynamics in semiconductors studied with time-resolved terahertz spectroscopy," *Rev. Mod. Phys.*, vol. 83, no. 2, pp. 543–586, 2011.
- [21] U. W. Kim, S. J. Oh, I. Maeng, C. Kang, and J.-H. Son, "Terahertz electrical characteristics of heavily doped n-GaAs thin films," *J. Korean Phys. Soc.*, vol. 50, no. 3, pp. 789–792, 2007.
- [22] S. Adachi, *Properties of Semiconductor Alloys: Group-IV, III-V and II-VI Semiconductors*, vol. 28. Hoboken, NJ, USA: Wiley, 2009.



**Satoshi Yamasaki** was born in Shimane Prefecture, Japan, in 1993. He received the B.E. degree in electrical and electronic engineering in 2016 from Tokyo Institute of Technology, Tokyo, Japan, where he is currently working toward the M.E. degree in electrical and electronic engineering.

His current research interests include optical-to-terahertz signal conversion.

Mr. Yamasaki is a student member of the Japan Society of Applied Physics.



**Akio Yasui** was born in Chiba Prefecture, Japan, in 1990. He received the B.E. degree in electrical engineering and the M.E. degree in electrical and electronic engineering from Tokyo University of Science, Tokyo, Japan, in 2014 and 2016, respectively.

He joined SoftBank Corporation in 2016. His research interests include the optical-to-terahertz signal conversion.



**Tomohiro Amemiya** (S'06–M'09) was born in Tokyo, Japan, in 1981. He received the B.S., M.S., and Ph.D. degrees in electronic engineering from the University of Tokyo, Tokyo, Japan, in 2004, 2006, and 2009, respectively.

In 2009, he moved to the Quantum Electronics Research Center, Tokyo Institute of Technology, as an Assistant Professor. Since 2016, he has been an Assistant Professor with the Institute of Innovative Research, Tokyo Institute of Technology.

His research interests include physics of photonic integrated circuits, metamaterials for optical frequencies, semiconductor light-controlling devices, and the technologies for fabricating these devices.

Dr. Amemiya is a member of the Optical Society of America, the American Physical Society, and the Japan Society of Applied Physics. He received the 2007 IEEE Photonics Society Annual Student Paper Award, the 2008 IEEE Photonics Society Graduate Student Fellowships, the 2012 Konica Minolta Imaging Award, the 2015 Yazaki Memorial Foundation Award, and the 2016 Young Scientists' Prize, the Commendation for Science and Technology by the Minister of Education, Culture, Sports, Science and Technology.

**Kentaro Furusawa** (M'03) received the B.S. and M.S. degrees in electronic engineering from Keio University, Minato, Japan, and the Ph.D. degree from Optoelectronics Research Centre, University of Southampton, Southampton, U.K., in 2003, where he worked on microstructured optical fibers and high power fiber lasers. Prior to joining National Institute of Information and Communications Technology in 2014, where he is currently a Senior Researcher, he experienced several positions in both academia and industry including a special Postdoctoral Fellow at RIKEN. His current research interests include micro/nanostructured optical devices and nonlinear guided-wave phenomena for frequency metrology applications. He is a member of the Optical Society of America.



**Shinsuke Hara** (M'13) received the B.E., M.E., and Ph.D. degrees in physics from Tokyo University of Science, Tokyo, Japan, in 2000, 2002, and 2005, respectively.

In 2013, he joined the National Institute of Information and Communication Technology, Koganei, Japan, as a Researcher. His research interests include millimeter wave CMOS circuits design and nanoscale semiconductor devices.



**Issei Watanabe** received the B.E., M.E., and Ph.D. degrees in engineering science from Osaka University, Suita, Japan, in 1999, 2001, and 2005, respectively. From 2001 to 2004, he joined collaboration team among Osaka University, Communications Research Laboratory (CRL) and Fujitsu Laboratories Limited, where he worked on growth of epitaxial heterostructure by MBE and fabrication and characterization of cryogenically cooled InP-based InGaAs/InAlAs HEMTs. In 2004, he joined the National Institute of Information and Communications

Technology (NICT, former CRL), Tokyo, Japan, where he has been involved in the research and development of nanoscale gate compound semiconductor electron devices and circuits, and high-frequency measurement technology for millimeter- and THz-wave applications.

He is a member of the Japan Society of Applied Physics and the Institute of Electronics, Information and Communication Engineers (IEICE).



**Atsushi Kanno** (M'11) received the B.S., M.S., and Ph.D. degrees in science from the University of Tsukuba, Tsukuba, Japan, in 1999, 2001, and 2005, respectively. In 2005, he was with the Venture Business Laboratory of the Institute of Science and Engineering, University of Tsukuba. In 2006, he joined the National Institute of Information and Communications Technology, Japan. His research interests include microwave/millimeter-wave/terahertz photonics, ultrafast optical and radio communication systems, lithium niobate optical modulators, and ultrafast phenomena in semiconductor optical devices.

Dr. Kanno is a member of the Institute of Electronics, Information and Communication Engineers (IEICE), the Japan Society of Applied Physics (JSAP), the Laser Society of Japan.



**Norihiko Sekine** (M'01) received the B.S., M.S., and Ph.D. degrees in electronic engineering from the University of Tokyo, Tokyo, Japan, in 1994, 1996, and 1999, respectively.

After acquiring industry experience, he is currently a Research Manager with the National Institute of Information and Communications Technology. His research interests include the physical properties of semiconductor nanostructures in the THz regime and their application to THz devices.

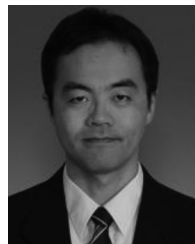
Dr. Sekine is a member of the Japan Society of Applied Physics, the Institute of Electronics, Information, and Communication Engineers, and the Institute of Electrical and Electronic Engineers.



**Zhichen Gu** was born in Shanghai, China, in 1991. He received the B.E. degree in communications engineering from Donghua University, Shanghai, China, in 2012, and the M.E. degree in electrical and electronic engineering from Tokyo Institute of Technology, Tokyo, Japan, in 2015. He is currently working toward the Ph.D. degree in the Department of Electrical and Electronic Engineering, Tokyo Institute of Technology.

His current research interests include membrane-based photonic devices for optical interconnection.

Mr. Gu is a student member of the Institute of Electronics, Information and Communication Engineers and the Japan Society of Applied Physics.



**Akifumi Kasamatsu** received the B.E., M.E., and Ph.D. degrees in electronics engineering from Sophia University, Tokyo, Japan, in 1991, 1993, and 1997, respectively.

From 1997 to 1999, he was an Assistant with Sophia University. From 1999 to 2002, he was with Fujitsu Laboratories, Ltd., Atsugi, Japan. Since 2002, he has been with the National Institute of Information and Communications Technology, Koganei, Japan, where he is currently an Executive Researcher and a Principal Investigator of the Terahertz Wave Electronics Project.

His current research interests include wireless communication technology, such as wireless transceivers and nanoscale semiconductor devices for millimeter wave and terahertz wave communications.



**Nobuhiko Nishiyama** (M'01–SM'07) was born in Yamaguchi Prefecture, Japan, in 1974. He received the B.E., M.E., and Ph.D. degrees from Tokyo Institute of Technology, Japan, in 1997, 1999, and 2001, respectively.

During his Ph.D. work, he demonstrated single-mode 0.98 and 1.1  $\mu\text{m}$  VCSEL arrays with stable polarization using misoriented substrates for high-speed optical networks as well as MOCVD-grown GaInNAs VCSELs. He joined Corning, Inc., New York, in 2001 and worked with the Semiconductor

Technology Research Group. At Corning, he worked on several subjects, including short-wavelength lasers, 1060-nm DFB/DBR lasers, and long-wavelength InP-based VCSELs. Since 2006, he has been an Associate Professor with Tokyo Institute of Technology. His current main interests include transistor lasers, silicon photonics, III–V silicon hybrid optical devices, and terahertz-optical signal conversions involving optics–electronics–radio integration circuits.

Dr. Nishiyama is a member of the Japan Society of Applied Physics, IEICE, and the IEEE Photonics Society. He received the Excellent Paper Award from the Institute of Electronics, Information and Communication Engineers of Japan in 2001, the Young Scientists' Prize in the Commendation for Science and Technology from the Minister of Education, Culture, Sports, Science and Technology in 2009, and the Ichimura Prize in Science for Distinguished Achievement in 2015.



**Shigehisa Arai** (M'83–SM'06–F'10) was born in Kanagawa Prefecture, Japan, in 1953. He received the B.E., M.E., and D.E. degrees in electronics from Tokyo Institute of Technology, Tokyo, Japan, in 1977, 1979, and 1982, respectively. During his Ph.D. work, he demonstrated room-temperature CW operations of 1.11–1.67  $\mu\text{m}$  long-wavelength lasers fabricated by liquid-phase epitaxy as well as their single-mode operations under rapid direct modulation.

He joined the Department of Physical Electronics, Tokyo Institute of Technology, as a Research Associate in 1982, and joined AT&T Bell Laboratories, Holmdel, NJ, USA, as a Visiting Researcher from 1983 to 1984, on leave from the Tokyo Institute of Technology. Further, he became a Lecturer in 1984, an Associate Professor in 1987, and a Professor with the Research Center for Quantum Effect Electronics and the Department of Electrical and Electronic Engineering in 1994. Since 2004, he has been a Professor with the Quantum Nanoelectronics Research Center, Tokyo Institute of Technology.

His research interests include photonic integrated devices such as dynamic-single-mode and wavelength-tunable semiconductor lasers, semiconductor optical amplifiers, and optical switches/modulators. His current research interests include studies of low-damage and cost-effective processing technologies of ultrafine structures for high-performance lasers and photonic integrated circuits on silicon platforms.

Dr. Arai is a member of the Optical Society of America, the Institute of Electronics, Information and Communication Engineers (IEICE), and the Japan Society of Applied Physics (JSAP). He received the Excellent Paper Award from the IEICE of Japan in 1988, the Michael Lunn Memorial Award from the Indium Phosphide and Related Materials Conference in 2000, Prizes for Science and Technology in the Commendation for Science and Technology from the Minister of Education, Culture, Sports, Science and Technology in 2008, an Electronics Society Award and the Achievement Award from IEICE in 2008 and 2011, respectively, a JSAP Fellowship in 2008, and SSDM Award from the International Conference on Solid-State Devices and Materials in 2016.